Supplementary Material

"A single neural network for cone-beam computed tomography-based radiotherapy of head-and-neck, lung and breast cancer"

Abstract

This file contains the supplementary material reporting: a collection of patient demographics 1, the imaging protocols 2, a description of the network architecture adopted 3, an overview of additional metric for the image comparison 4, and images for further patients 5.

1. Patient demographics

Sex, age, tumour type, tumour stage, dose prescription in terms of total dose, fractionation scheme, linac on which the CBCT have been acquired and number of days between the acquisition of CBCT and CT were reported for all the patients in the training, validation and test set for head-and-neck (Table S1), breast (Table S2) and lung (Table S3). The gender is expressed as male (M) or female (F). The tumour type can be accompanied by the specification of the location of the tumour, e.g. right (R) or left (L). Also, the follwoing abbreviations have been introduced: SupraClav for supra clavicularis, local or locoreg for local and loco-regional treatment. In the prescription SIB stands for simultaneous integrated boost; boost indicates a sequential boost, adjuv if treatment is intended as an adjuvant therapy, reirr in the case of reirradiation, pall in case of palliative treatment, lymph when elective irradiation was considered. Other abbreviations are reported in the caption of each table. For the patients in the training set, the CBCT have been the closest to CT or rCT. For the patients in the test set, the RT plan was briefly described in terms of angle of the beam and the arc of irradiation for intensity-modulated radiotherapy (IMRT) and volumetric modulated arc therapy (VMAT). Also, the volumetric percentage difference of the body between rCT (ΔV_{rCT}) and sCT (ΔV_{sCT}) to CT in $\mathrm{Mask}_{\mathrm{CBCT}}$ was reported.

Table S 1: Overview of the patient demographic for the **head-and-neck** cancer patients split in training, validation and test set.

Set	Pt no.	Sex	Age [y]	Tumour	Stage [TNM]	Prescription	Frac no.	Dose per frac. [Gy]	Plan*	Linac	CBCT-to-(r)CT [d]	rCT-to-CT [d]	ΔV_{rCT} [%]	ΔV_{sCT} [%]
Training	H1	M	60.4	Oropharynx R	T3N2b	70Gy SIB	35	2.0		U09	3			
	H2	M	67.3	Larynx glottid	cT1aN0	60Gy	25	2.4		U11	1			
	H3	M	48.1	Tongue R	pT4aN2b	66Gy SIB	33	2.0		U14	3			
	H4	M	68.6	Larynx	pT4cN0	66Gy SIB	33	2.0		U14	32			
	H5	M	62.7	Nasopharynx	cTxN2cMx	70Gy SIB	35	2.0		U14	0			
	H6	M	58.6	Nasopharynx	T1N2	70Gy SIB	35	2.0		U11	4			
	H7	M	71.6	Oropharynx	T2N3	70Gy	35	2.0		U14	1			
	H8	M	54.5	Oropharynx	T4aN2cM0	46Gy, boost 70Gy	23	2.0		U14	2			
	H9	M	53.6	Tonsil	T2N2aM0	70Gy SIB	35	2.0		U11	0			
	H10	M	69.7	Parotis L (meths SCC)	T4NxM1	66Gy adjuv	33	2.0		U14	4			
	H11	M	49.0	Oropharynx R	cT1cN2acM0	70Gy SIB	35	2.0		U09	3			
	H12	M	66.8	Oropharynx (tonsil)	cT2N2b	70Gy SIB	35	2.0		U11	2			
	H13	F	70.5	Parotis L	T1aN0	50Gy	25	2.0		U14	4			
	H14	F	61.3	Hypopharynx R	T2N1M0	46Gy SIB	23	2.0		U14	5			
	H15	F	52.3	Nasopharynx	cT3N2bM0	46Gy SIB	23	2.0		U14	2			
Validation	H16	M	74.6	Tonguebasis	T4N2c	70Gy SIB	35	2.0		U14	0	261		
	H17	M	67.3	SupraClav R	cT4N3M1	16Gy reirr	2	8.0		U05	0			
	H18	F	54.3	Hypopharynx axilla R	cT1N3M1	70Gy	35	2.0		U14	10	34		
	H19	M	85.6	Tonsil epiglottis	T2N1	69Gy	30	2.3		U11	12	121		
	H20	M	74.5	Non-Hodgkin Lymph SupraClav L	Deauville V	30Gy pall	10	3.0		U12	3			
	H21	M	67.3	Tongue R	cT1N2bM1	48Gy prim + lymph	16	3.0		U12	16			
	H22	F	53.5	Hypopharynx	T4a	70Gy SIB	35	2.0		U12	-6	32		
	h23	F	71.4	Head L	cT3N2M1b	20Gy pall reirr	5	4.0		U05	4			
Test	H24	M	71.4	Hypopharynx L	T4aN2b	70Gy SIB	35	2.0	360°	U09	55	56	-7.8	-8.0
	H25	M	64.0	Head R	T3N1	46Gy	23	2.0	360°	U11	47	47	-9.7	-9.6
	H26	M	67.3	Supraglottis	T2N0M0	70Gy SIB	35	2.0	360°	U14	63	64	-6.6	6.1
	H27	F	74.7	Parotis L	pT3N2b	47Gy SIB	15	1.8	360°	U14	16	20	-3.1	-3.0
	H28	M	55.3	Oropharynx	T2N0M0	70Gy SIB	12/35	2.0	180°	U15	53	49	-2.7	-3.3
	H20	M	62.0	Oropharynx	cT4aN2c	47Gy SIB	15	1.8	180°	U12	44	44	-4.0	-4.6
	H30	M	61.2	Parotis R	cT0N2aM0	69Gy	3/33	2.3	170°	U11	43	35	-1.8	-2.3
	H31	M	52.0	Oropharynx L tongue L	cT4N3bM0	70Gy SIB	35	2.0	360°	U10	39	34	-0.3	-1.1
	H32	F	53.7	Mouth bed	pT4acN0M0	70Gy adjuv	12/35	2.0	170°	U14	67	62	1.6	1.5
	H33	M	75.5	Glottis Larynx R	cT2N0M0	70Gy	35	2.0	360°	U10	34	34	-8.0	-8.3

*VMAT plans with 6 MV energy were generally delivered plans indicates the degree of the arc.

Abbreviations: R = right; L = left; SIB = simultaneous integrated boost; reirr = reirradiation; pall = palliation; adjuv = adjuvant therapy; SupraClav = supra clavicular; SCC = squamous cell carcinoma; lymph = lymphonode irradiation; ΔV_{rCT} = percentage difference of the volume in $\mathrm{Mask}_{\mathrm{CBCT}}$ of the body calculated in rCT respect to CT; ΔV_{rCT} = percentage difference of the volume in $\mathrm{Mask}_{\mathrm{CBCT}}$ of the body calculated in sCT respect to CT.

Table S 2: Overview of the patient demographic for **breast** cancer patients split in training, validation and test set.

Set	Pt no.	Sex	Age [y]	Tumour	Stage [TNM]	Prescription	Frac no.	Dose per frac. [Gy]	Plan*	Linac	CBCT-to-(r)CT [d]	rCT-to-CT [d]	ΔV_{rCT} [%]	ΔV_{sCT} [%]
Training	B1	F	57.6	R	cT2-3N2M0	42.56Gy	16	2.66		U10	0			
	B2	F	33.3	L locoreg	cT3N1M0	61.2Gy SIB + lymph	23	2.66		U12	1			
	B3	F	46.6	R local	pT1cN1	46Gy SIB	21	2.66		U12	5			
	B4	F	52.2	R local	cT2N0M0	46Gy SIB	21	2.66		U11	2			
	B5	F	45.8	R	cT2N0M0	46Gy SIB	21	2.66		U05	5			
	B6	F	63.3	R locoreg	cT2N1M0	46Gy	21	2.66		U14	4			
	B7	F	59.5	R	pT2N0	42.56Gy reirr	16	2.66		U04	5			
	B8	F	84.9	R	pT2N3M0	61.2Gy SIB	23	2.66		U11	2			
	B9	F	60.0	R	cT2N2M0	46Gy SIB	21	2.66		U04	4			
	B10	F	66.7	L locoreg	cT2N2M0	42.56Gy	16	2.66		U11	5			
	B11	F	67.1	R	pT1G2N0	42.56Gy	16	2.66		U04	1			
	B12	F	69.4	L local	cT2N0Mx	46Gy SIB + 21x0.5 seq	21	2.66		U11	4			
	B13	F	93.7	R	pT1N1	24Gy pall	3	8.00		U04,U10	2			
	B14	F	67.7	R	cT2-3N2M0	42.56Gy	16	2.66		U04,U07	4			
	B15	F	37.1	R	cT1N0	46Gy SIB	21	2.66		U04	4			
Validation	B16	F	56.5	R postop	pT1N0	55.86Gy SIB	21	2.17		U10	14	/		
	B17	F	57.2	Thorax	T23	45.57 local	21	2.17		U12	-7	54		
	B18	F	63.5	R	cT2pN1M0	46Gy SIB neo-adjuv chemo	23	2.66		U04	7	49		
	B19	F	69.5	R preop	pT1aN0	42.56Gy	16	2.66		U04	38	27		
	B20	F	70.0	L	pT4N0	60Gy SBRT	5	12.00		U09	47	187		
	B21	F	67.7	R postop	cT2-3N2M0	42.56Gy adj	16	2.66		U04,U07	1	44		
	B22	F	52.4	R	pT1cG2N1	42.56Gy	16	2.66		U05	7	9-25		
	B23	F	67.6	L	cT1cN0	15/20Gy SIB	1	20.00		U10	8			
Test	B24	F	76.8	R postop	pT1cN0	61.2Gy SIB	23	2.66	6MV 8f*	U04	14	14	3.6	6.8
	B25	F	50.3	L postop	pT1N0	61.2Gy SIB	23	2.66	10MV 7f*	U14	26	26	5.4	5.5
	B26	F	72.2	L postop	pT1cG2N1	42.56Gy lymph	16	2.66	10MV 4f*	U08	16	14	3.5	3.6
	B27	F	77.3	L local	pT3N1	61.2Gy SIB	23	2.66	6/10MV 4/8f*	U14	23	22	-3.5	2.7
	B28	F	43.8	R Thoraxwand locoreg	cT2mN3bM0	42.56Gy	16	2.66	10MV 270°	U14	8	11	-1.0	-0.4
	B29	F	74.1	R locoreg	pT1cpN2	42.56Gy lymph	16	2.66	6/10MV 2/9f*	U04	21	21	-1.6	-1.7
	B30	F	57.8	L local	cT2N1M0	42.56Gy	16	2.66	10MV 10f*	U11	17	17	8.3	9.3
	B31	F	72.2	L postop	pT1cG2N1	42.56Gy lymph	16	2.66	6MV 220°	U11	14	12	-2.8	-2.7
	B32	F	39.2	L	pT1cN0M0	40.05Gy	15	2.67	6MV 240°	U12	20	20	-8.2	-13.9
	B33	F	42.3	L postop	cT1bN0/1	40.05Gy	15	2.67	6/10MV 4/5f*	U12	31	28	0.9	-0.4

* f = fields/beams of IMRT; if f is not indicated, a VMAT plan was delivered and the arc range is expressed in degree. Abbreviations: R = right; L = left; SIB = simultaneous integrated boost; reirr = reirradiation; pall = palliation; (neo) adjuv = (neo)adjuvant therapy; chemo = chemotherapy; seq = sequential; local = local treatment; locoreg = locoregional treatment; postop = postoperative irradiation; lymph = lymphonode irradiation; ΔV_{rCT} = percentage difference of the volume in $\mathrm{Mask_{CBCT}}$ of the body calculated in rCT respect to CT; ΔV_{rCT} = percentage difference of the volume in $\mathrm{Mask_{CBCT}}$ of the body calculated in sCT respect to CT.

Table S 3: Overview of the patient demopgraphic for the **lung** cancer patients split in training, validation and test set.

Set	Pt no.	Sex	Age [y]	Tumour	Stage [TNM]	Prescription	Frac no.	Dose per frac. [Gy]	Plan*	Linac	CBCT-to-(r)CT [d]	rCT-to-CT [d]	ΔV_{rCT} [%]	ΔV_{sCT} [%]
Training	L1	F	55.2	R NSCLC R	cT4N2M1a	16Gy pall	2	8.00		U05	0			
	L2	F	77.8	NSCLC R	pT2bN3M1a-b	8Gy pall	1	8.00		U05	0			
	L3	M	80.5	R	T4	8Gy pall	1	8.00		U04	0			
	L4	F	52.7	R NSCLC recidive	T4	8Gy pall	1	8.00		U05,U03	0			
	L5	F	59.5	Adenocarc postop	T4N1M1	30Gy	10	3.00		U04,U05	18			
	L6	F	59.9	Meths	T2-3	30Gy	10	3.00		U09,U05	4			
	L7	F	60.3	Adenocarc R	pT1N0Mo	60Gy SBRT	5	12.00		U09	2			
	L8	F	61.2	R + meths	T2-3	30Gy	10	3.00		U09	4			
	L9	M	69.8	R Thoraxwand	T4N2M1c	8Gy	1	8.00		U04	0			
	L10	M	65.1	L	pT4aN0M0	8Gy reirr	1	8.00		U05	1			
	L11	M	55.7	L NSCLC	T4	20Gy	5	4.00		U11	1			
	L12	M	83.9	L NSCLC	cT4N0Mo	39Gy	13	3.00		U09,U14	1			
	L13	M	60.6	L NSCLC	cT4N1M1c	8Gy pall	1	8.00		U05	0			
	L14	M	63.3	SCLC	cT2N2M0	39Gy	13	3.00		U09	3			
	L15	M	59.7	R NSCLC	cT4N4M1a	8Gy pall	1	8.00		U05	0			
Validation	L16	M	70.6	Mediastinum	pT4N2M0	65Gy	25	3.00		U12	-25	36		
	L17	M	59.4	R NSCLC	cT4N3M1	48Gy	16	3.00		U9	-9	13		
	L18	M	62.5	L SCLC	cT3N3M0	45 Gy SIB	15	5.00		U12	0	78		
	L19	M	59.8	L NSCLC	T4	16Gy pall	2	8.00		U09	5	/		
	L20	M	74.4	L SCLC	T4	8Gy	1	8.00		U04	0	159		
	L21	M	56.5	R NSCLC local	pT3N1M0	54 Gy pall	3	18.00		U12	11	/		
	L22	F	8.9	Wilms, both	T1	12Gy+22Gy SIB	8	1.5+2.75		U15	14	/		
	L23	M	63.2	L	cT2N2M0	60Gy SBRT	8	7.50		U15	24	25		
Test	L24	M	64.0	Adenocarc	cT1cN2M0	65Gy	25	2.60	10MV 195°	U11	27	28	2.5	-1.8
	L25	F	60.9	NSCLC	cT2N3M0	65 Gy	25	2.60	10MV 195°	U10	21	21	-4.2	-2.3
	L26	F	67.0	L SCLC	cT4N3M1c	30Gy SABRT	10	3.00	10MV 195°	U14	11	11	5.3	-0.3
	L27	M	81.7	L locoreg	T4N2M0	36Gy SABRT	12	3.00	10MV 195°	U12	12	14	-2.6	-5.8
	L28	M	82.3	R	cT1aN0M0	65Gy	25	2.60	10MV 195°	U14	23	23	-1.4	0.0
	L29	F	57.5	Adenocarc R	T2N4	60Gy SABRT	5	12.00	6MV 360°	U04	27	27	1.3	2.8
	L30	M	63.3	SCLC	cT2N2M0	66Gy	33	2.00	10MV 195°	U09	8	12	2.9	3.4
	L31	M	81.8	Adenocarc R	c3T3N3M0	3Gy pall	10	3.0	10MV 2f*	U14	-47	-49	0.4	1.1
	L32	F	73.1	R NSCLC	T3N2M0	65Gy	25	2.60	10MV 195°	U15	14	16	-1.1	-1.4
	L33	F	60.8	L NSCLC	T4N1M0	65Gy	25	2.60	10MV 195°	U08	22	24	0.4	0.5

* f = fields/beams of IMRT; if f is not indicated, a VMAT plan was delivered and the arc range is expressed in degree. Abbreviations: R = right; L = left; both = both lungs were irradaited; SIB = simultaneous integrated boost; NSCLC = Non-small-cell lung carcinoma; SCLC = Small-cell lung carcinoma; reirr = reirradiation; pall = palliation; SABRT = stereotactic ablative radiotherapy; SBRT = stereotactic body radiation therapy ; postop = postoperative irradiation; adenocarc = adenocarcinoma; ΔV_{rCT} = percentage difference of the volume in $\mathrm{Mask}_{\mathrm{CBCT}}$ of the body calculated in rCT respect to CT; ΔV_{rCT} = percentage difference of the volume in $\mathrm{Mask}_{\mathrm{CBCT}}$ of the body calculated in sCT respect to CT.

2. Imaging Protocols

CTs were acquired on a Brilliance Big Bore (Philips Healthcare, Ohio, USA); CBCTs were acquired using X-ray volumetric imaging (XVI, v5.0.2b72 Elekta AB, Sweden) system. Table 4 reports the imaging protocols for CT, rescan CT (rCT) and CBCT for all the patients included in the study in terms of field-of-view (FOV), acquisition matrix (Acq matrix), resolution (Res), tube voltage (kVp), exposure (ms) and current (mA). CBCTs were acquired with 0.25 rotation/s gantry speed and 5.5 frames/s. All the CBCTs were acquired with a 200°-arc utilising an empty filter cassette (F0) in combination with a centred detector panel (S position, maximum FOV=27x27 cm^2). The field-of-view (FOV) was in four cases (elective lymph-nodes irradiations or double-sided irradiation for breast and HN patients) enlarged to a maximum of 41x41 cm^2 using a shifted detector panel (M position) to accommodate the CTV in the CBCT FOV. Imaging frequency of CBCT followed the extended non-action limit protocol [1]: online corrections (action level 0 mm) were applied in the case of partial or ablative breast irradiation, and offline long (imaging the first three days and then every five) scheme were applied for irradiations having ≥ 20 and short scheme (imaging the first two days and then every two) for < 20 fractions. Imaging frequency may have been increased after consultation between a medical physicist and a radiotherapist on a single patient-basis in case large inter-fraction motions were observed in the initial fractions or whenever RT technicians reported difficulties in reproducing the planning position.

Clinical set-up corrections were estimated within a clip-box including the CTV based on bone rigid (translation and rotation) matching [2]. For the breast patients treated with local RT followed by a sequential boost, a dual rigid registration was performed based first on bone matching followed by grey level (soft-tissue) matching [3, 4]. The centre of rotation was assigned as the centre of the PTV. In all cases, the set-up correction finally applied consisted of sole translation, trying to minimise the effect of rotations previously estimated.

Table S 4: Overview of CT (including also rescan (r)CT) and CBCT imaging protocols in terms of field-of-view (FOV), acquisition matrix (Acq matrix), resolution (Res), tube voltage (kVp), exposure (ms) and current (mA). For exposure and current, the mean value ($\pm\sigma$) was reported along with the range.

Modality	**Site**	**FOV**[a] [cm^3]	**Acq matrix**[a]	**Res**[a] [mm^3]	**Voltage**[b] [kVp]	**Exposure**[b] [ms]	**Current**[b] [mA]
(r)CT	Head-and-neck	43-70	512	0.83-1.37	120	983±65	159±50
		43-70	512	0.83-1.37		923-1090	47-271
		30-111	101-535	2-3			
	Breast	47-70	512	0.92-1.37	120	1050±109	63±37
		47-70	512	0.92-1.37		923-1332	31-271
		31-120	103-400	2-3			
	Lung	29-70	512	0.57-1.37	120	3886±3095	98±66
		29-70	512	0.57-1.37		500-10091	30-271
		23-220	76-660	1-3			
CBCT	Head-and-neck	27	135-270	1-2	100[c]	11±5	14±3
		27	135-270	1-2		10-40	10-20
		13-53	126-526	1-2			
	Breast	27-41	270-540	0.5-1	120	33±2	17±2
		27-41	270-540	0.5-1		32-40	16-20
		26-53	262-526	0.5-1			
	Lung	27	270	1-2	120[d]	31±6	20±1
		27	270	1-2		10-40	16-25
		26-53	128-528	1-2			

[a] Expressed in RL, AP, FH directions; the range is reported in terms of min-max.
[b] Reported in terms of mean value and range=min-max.
[c] Except for H18 and H20 where kVP was 120.
[d] Except for L11, L22 and L24 where kVP was 100.

3. Network architecture

The cycle-GAN employed in this study was constituted by nine blocks of residual networks [5] as generators and by Patch-GANs [6] as discriminators. Figure S1 shows the architecture of the generator and discriminator. Stochastic gradient descendent was used applying an Adam solver [7] with learning rate = 0.0002, momentum parameters $\beta_1 = 0.5$ and $\beta_2 = 0.999$. Instance normalisation [8] was employed with a batch size of 1. The weights of the network were randomly initialised from $\mathcal{N}(0, 0.02)$. Weight optimisation was performed as in Goodfellow et al. [9] alternating between one gradient descendent step on the discriminator network and one step on the generator network after having performed a forward and backward cycle. A structured loss function composed by GAN+$\lambda \cdot \mathcal{L}1$+cycle-consistency with $\lambda = 25$ was adopted. The original implementation of the network by Zhu et al [10][1] was modified to accommodate 16-bit grey-scale images with a size of 256x256.

Both networks were trained for 200 epochs on a Tesla P100 (16 Gb, NVIDIA, California, USA) graphical processing unit (GPU) with batch size one and image pool of 1000 images. Data augmentation was applied during training by flipping the images left and right and randomly cropping of 30x30 voxels after having bi-linearly resampled the images to 286x286 voxels in $\text{Mask}_{\text{CBCT}}$. Early stopping was applied controlling the average and σ of the $\mathcal{L}_1$ within the body contour over the patients of the validation set: we selected the first epoch with average $\mathcal{L}_1$ differing less than one σ compared to the following three epochs. Note that $\mathcal{L}_1$ was calculated at every 10 epoch (a total of 20 models were stored, one each 10 epochs).

4. Image Comparison

Table 5 reports the similarity between the intensity of sCT, CBCT, CT and rCT calculated within $\text{Mask}_{\text{CBCT}}$ in terms of peak signal-to-noise ratio (PSNR) and structural similarity index metric (SSIM) as proposed by Liang et al. [11].

Table S 5: Image comparison calculated as mean ($\pm 1\sigma$) and range ([min; max]) of the test dataset (30 patients) compared to the reference dataset in terms of peak signal-to-noise ratio (PSNR) and structural similarity index metric (SSIM) between the Test and the Ref images. Values are expressed in dB for the PSNR.

Site		**Head-and-Neck**		**Breast**		**Lung**	
Test	**Ref**	**PSRN**	**SSIM**	**PSNR**	**SSIM**	**PSNR**	**SSIM**
		[dB]		[dB]		[dB]	
CBCT	rCT	24.6±0.8	0.46±0.05	25.3±1.8	0.71±0.04	23.7±1.4	0.69±0.04
		[23.1;26.1]	[0.38;0.52]	[22.2;28.1]	[0.63;0.75]	[22.2;26.7]	[0.58;0.73]
sCT$^+$	rCT	30.5±2.2	0.81±0.04	29.0±2.1	0.76±0.02	28.5±1.6	0.78±0.04
		[27.0;33.4]	[0.75;0.88]	[26.0;32.3]	[0.72;0.79]	[25.6;31.3]	[0.72;0.88]
sCT*	rCT	30.6±2.2	0.80±0.04	28.8±2.0	0.80±0.04	28.4±1.4	0.78±0.05
		[27.1;33.7]	[0.74;0.85]	[25.7;31.8]	[0.74;0.85]	[26.1;31.1]	[0.72;0.87]
CT	rCT	27.9±1.9	0.86±0.04	28.2±2.3	0.85±0.05	27.0±1.9	0.77±0.06
		[25.3;30.5]	[0.80;0.92]	[23.6;30.7]	[0.74;0.90]	[23.5;29.5]	[0.63;0.83]

$^+$ sCT obtained from a single network trained on all the anatomical sites.
* sCT obtained from three different networks trained on each anatomical site.

5. Single patient overview

In the following pages are shown CBCT, CT, rCT and sCT as well as the image differences to CT, dose, dose differences and DVH for the patients in the test set for whom analysis of DVH-points reported dose

[1] `https://github.com/xhujoy/CycleGAN-tensorflow`

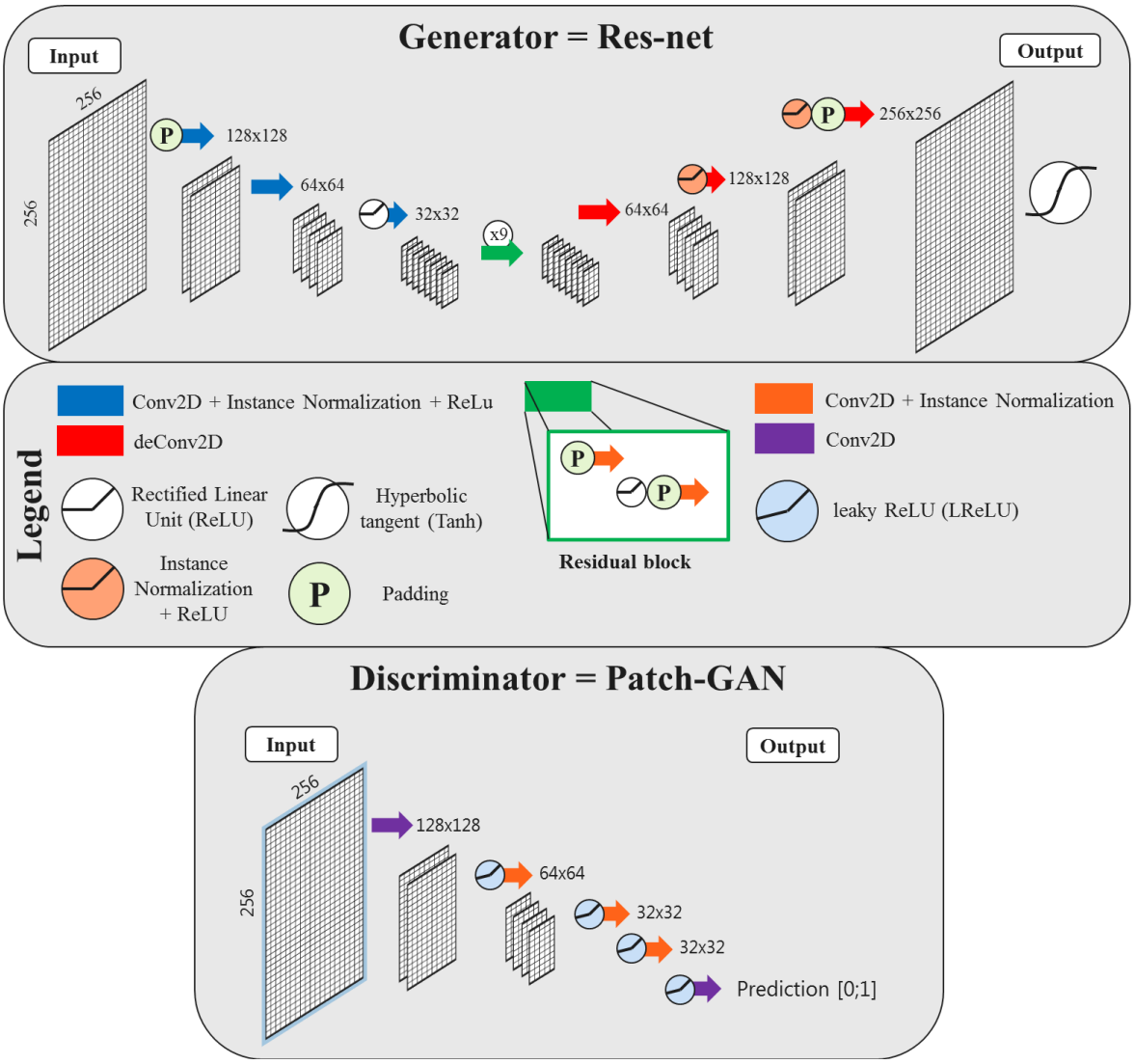

Figure S 1: Architecture of the nine-block residual network used as a generator (top) and of the convolutional network called Patch-GAN used as a discriminator. The size of the images is numerically reported, except for the residual block, where it remains stable. Note that the nine-blocks are omitted in the schematic, as well as the data-flow of the discriminator. Each of the filters had stride two, kernel size four; leaky rectilinear rectifier unit had a scalar multiplier of 0.2, padding was applied in reflect mode.

differences > 2% (L25, L27, B31). Multiple views (e.g. axial, sagittal or coronal) are presented according to which view was most representative to explain the differences reported.

Figure S2 reports images and doses for lung cancer patient L25 and and Figure S3 for L27. For both these patients, different respiratory phases can be noticed, e.g. looking at the lower border of the lungs. For L25, residual artefact characterised by inhomogeneous HUs seem to be present along the cranio-caudal direction in the lungs: it seems that, for this case, the CBCT artefacts were not fully corrected in the lungs. The image protocols were reconsidered for L25, and it was observed that this was the only patient acquired on the linac named "U10": no training data were present for lung patients from this linac. Besides, we hypothesise that data in the test may have been imbalanced compared to data in training set for what concern linacs, as it is discussed in the body of the manuscript.

For L27, one can observe that the CBCT was characterised by severe scatter artefacts probably because the patient was obese and the image protocol has not been optimised on a patient basis. In this case, bones on sCT were not entirely recovered, probably due to the low quality of CBCT.

In Figure S4 and S5, the anatomical differences due to residual set-up differences are visible for B30 and B31. Specifically, for B30, a bolus was used, and it is evident the anatomical mismatch and difference in bolus position between rCT and sCT.

References

[1] de Boer HC, Heijmen BJ. A protocol for the reduction of systematic patient setup errors with minimal portal imaging workload. Int J Radiat Oncol Biol Phys 2001;50:1350–65. 10.1016/S0360-3016(01)01624-8.

[2] Borgefors G. Hierarchical chamfer matching: a parametric edge matching algorithm. IEEE Transactions on Pattern Analysis and Machine Intelligence 1988;10:849–65. 10.1109/34.9107.

[3] Hristov DH, Fallone BG. A grey-level image alignment algorithm for registration of portal images and digitally reconstructed radiographs. Med Phys 1996;23:75–84. 10.1118/1.597743.

[4] Roche A, Malandain G, Pennec X, Ayache N. The correlation ratio as a new similarity measure for multimodal image registration. In: Lecture Notes in Computer Science, MICCAI. Springer, Berlin, Heidelberg; 1998, p. 1115–24. 10.1007/BFb0056301.

[5] Johnson J, Alahi A, Fei-Fei L. Perceptual Losses for Real-Time Style Transfer and Super-Resolution. Computer Vision ECCV 2016 2016;:694–71110.1007/978-3-319-46475-6_43.

[6] Isola P, Zhu JY, Zhou T, Efros AA. Image-to-Image Translation with Conditional Adversarial Networks. In: 2017 IEEE Conference on Computer Vision and Pattern Recognition (CVPR). IEEE. ISBN 978-1-5386-0457-1; 2017, p. 5967–76. https://doi.org/10.1109/CVPR.2017.632.

[7] Kingma DP, Ba J. Adam: A Method for Stochastic Optimization. arXiv preprint arXiv:14126980 2014;arXiv:1412.6980.

[8] Ulyanov D, Vedaldi A, Lempitsky V. Instance Normalization: The Missing Ingredient for Fast Stylization. arXiv preprint arXiv:160708022 2016;arXiv:1607.08022.

[9] Goodfellow I, Pouget-Abadie J, Mirza M, Xu B, Warde-Farley D, Ozair S, et al. Generative Adversarial Nets. In: Ghahramani Z, Welling M, Cortes C, Lawrence ND, Weinberger KQ, editors. Advances in Neural Information Processing Systems 27. Curran Associates, Inc.; 2014, p. 2672–80.

[10] Zhu JY, Park T, Isola P, Efros AA. Unpaired image-to-image translation using cycle-consistent adversarial networks. In: 2017 IEEE International Conference on Computer Vision (ICCV). Venice: IEEE; 2017, p. 2242–51. URL: https://doi.org/10.1109/ICCV.2017.244.

[11] Liang X, Chen L, Nguyen D, Zhou Z, Gu X, Yang M, et al. Generating synthesized computed tomography (CT) from cone-beam computed tomography (CBCT) using CycleGAN for adaptive radiation therapy. Phys Med Biol 2019;64:125002. https://doi.org/10.1088/1361-6560/ab22f9.

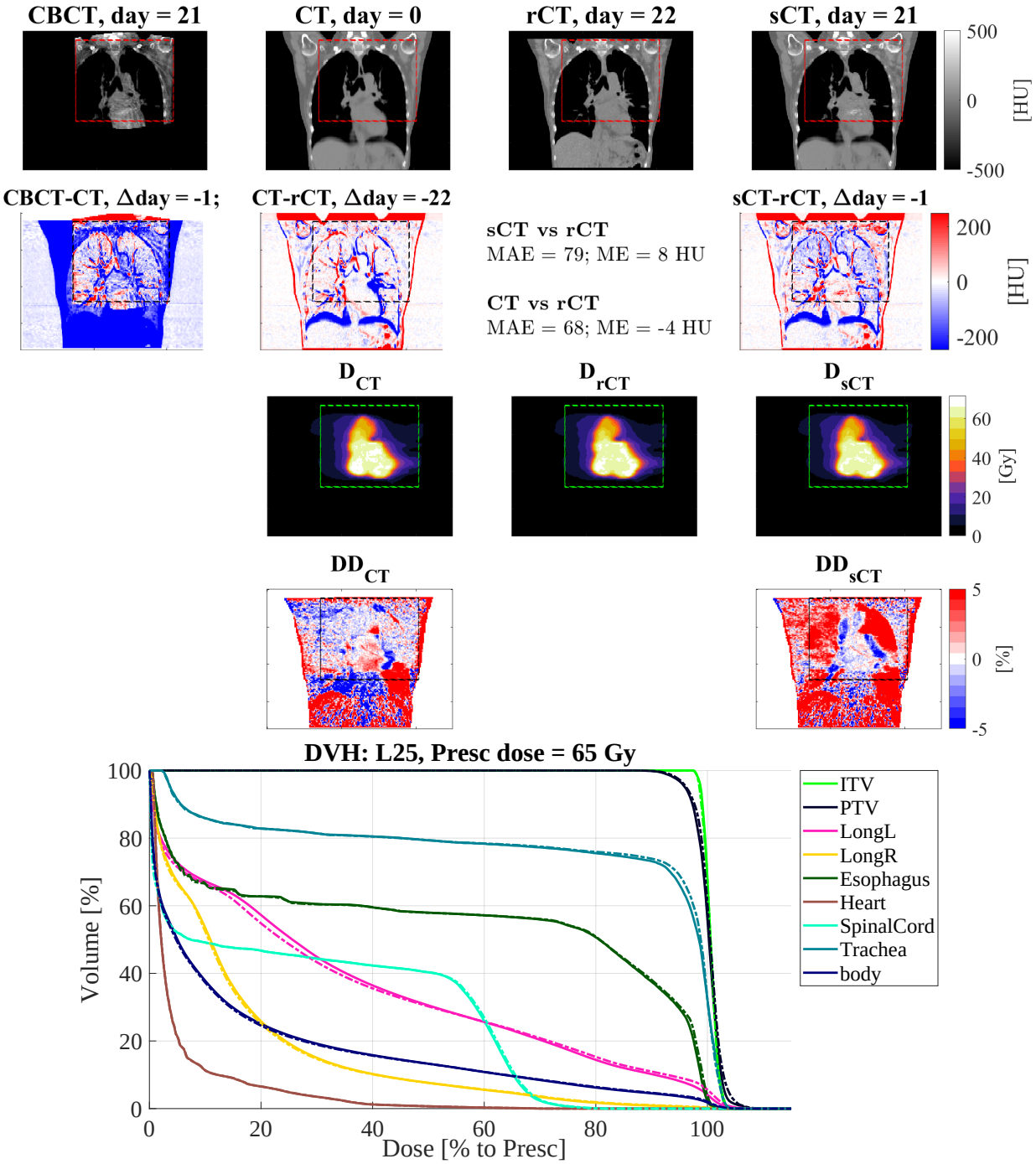

Figure S 2: Coronal views for the lung cancer patient L25 of: (1^{st} row) CBCT (1^{st} column), CT (2^{nd} column), rescan CT (rCT, 3^{rd} column) and synthetic CT (sCT, 4^{th} column), along with (2^{nd} row) the respective difference to rCT, and the doses (3^{rd} row) and the relative dose differences (4^{th}). The red, black, or green dotted rectangles indicate the position of $\text{Mask}_{\text{CBCT}}$. The days refer to the acquisition date relative of the planning CT. In the 5^{th} row, the DVH is shown for target and OARs of sCT (solid lines) and rCT (dashed lines).

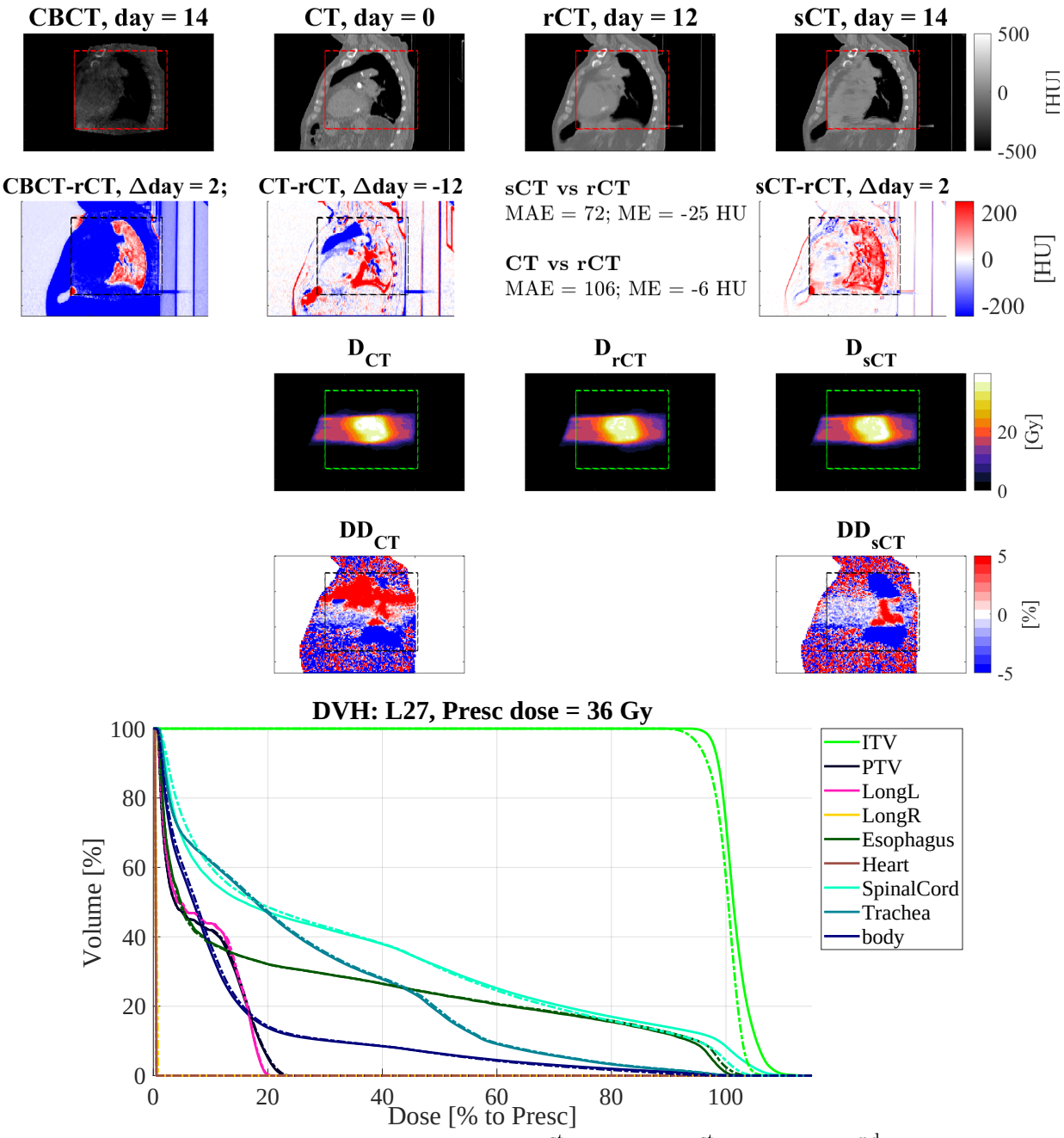

Figure S 3: Sagittal views for the lung cancer patient L27 of: (1^{st} row) CBCT (1^{st} column), CT (2^{nd} column), rescan CT (rCT, 3^{rd} column) and synthetic CT (sCT, 4^{th} column), along with (2^{nd} row) the respective difference to rCT, and the doses (3^{rd} row) and the relative dose differences (4^{th}). The red, black, or green dotted rectangles indicate the position of $\text{Mask}_{\text{CBCT}}$. The days refer to the acquisition date relative of the planning CT. In the 5^{th} row, the DVH is shown for target and OARs of sCT (solid lines) and rCT (dashed lines).

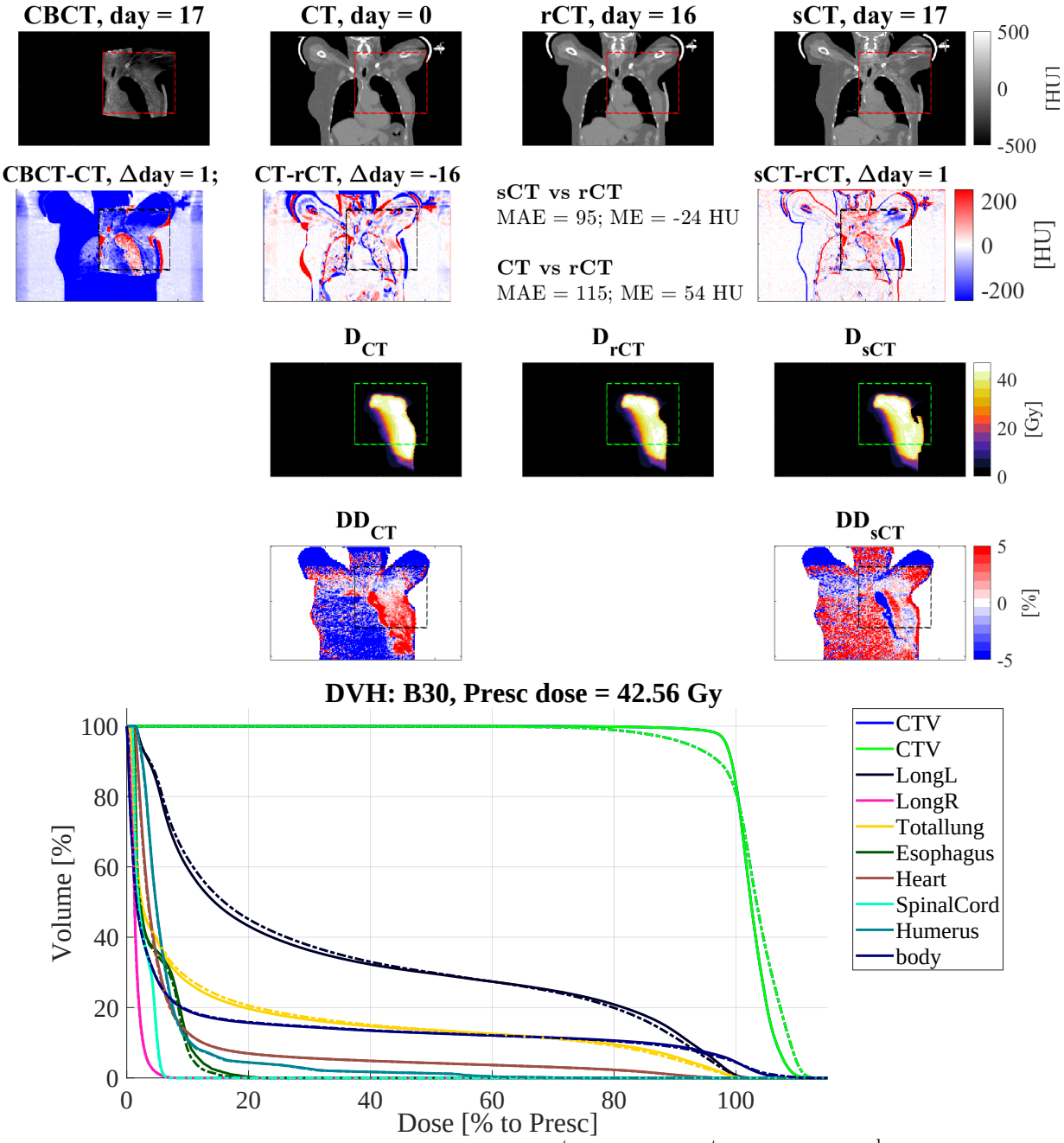

Figure S 4: Coronal views for the breast cancer patient B30 of: (1^{st} row) CBCT (1^{st} column), CT (2^{nd} column), rescan CT (rCT, 3^{rd} column) and synthetic CT (sCT, 4^{th} column), along with (2^{nd} row) the respective difference to rCT, and the doses (3^{rd} row) and the relative dose differences (4^{th}). The red, black, or green dotted rectangles indicate the position of $\text{Mask}_{\text{CBCT}}$. The days refer to the acquisition date relative of the planning CT. In the 5^{th} rows, the DVH is shown for target and OARs of sCT (solid lines) and rCT (dashed lines).

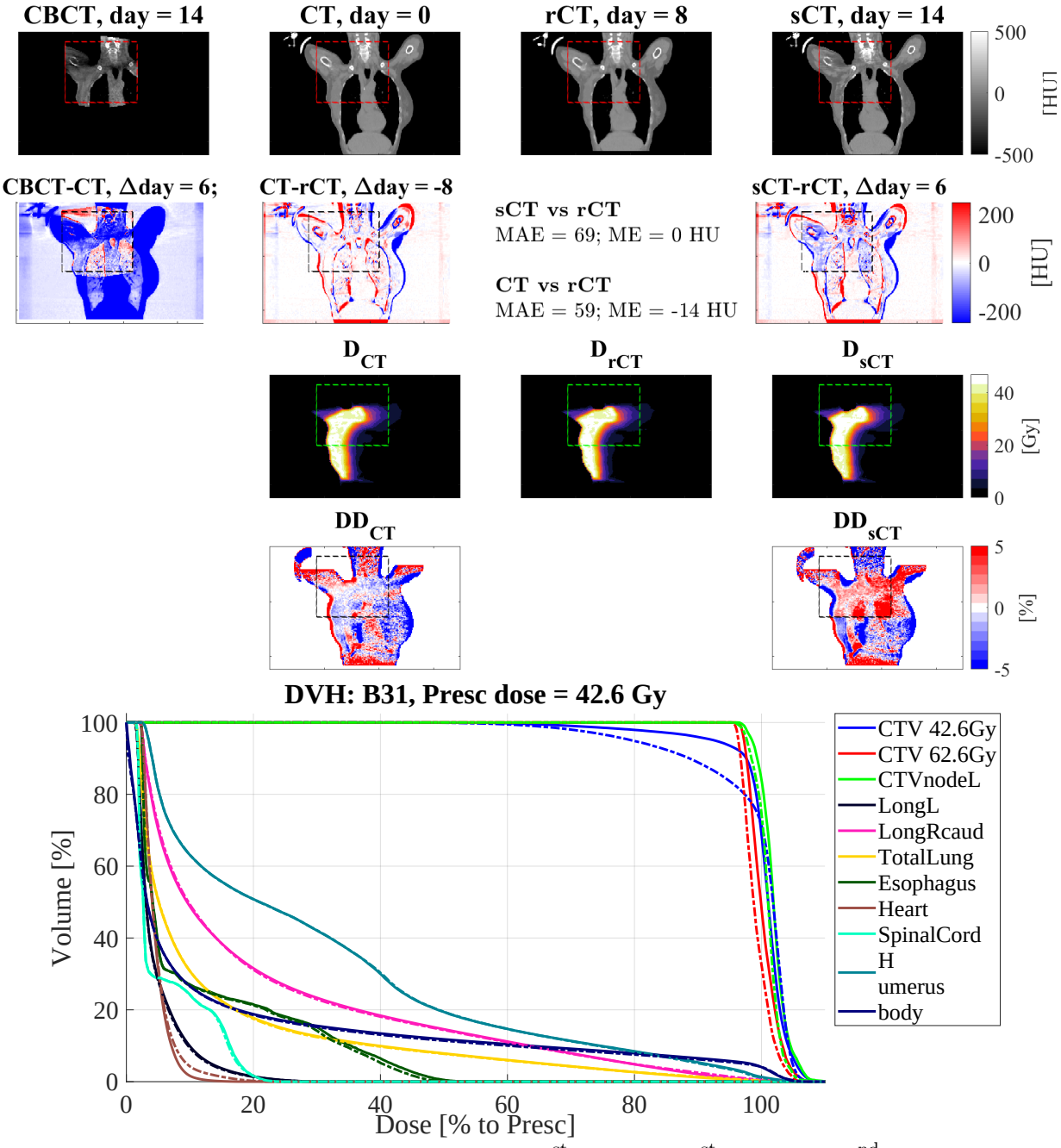

Figure S 5: Coronal views for the breast cancer patient B31 of: (1^{st} row) CBCT (1^{st} column), CT (2^{nd} column), rescan CT (rCT, 3^{rd} column) and synthetic CT (sCT, 4^{th} column), along with (2^{nd} row) the respective difference to rCT, and the doses (3^{rd} row) and the relative dose differences (4^{th}). The red, black, or green dotted rectangles indicate the position of $\text{Mask}_{\text{CBCT}}$. The days refer to the acquisition date relative of the planning CT. In the 5^{th} rows, the DVH is shown for target and OARs of sCT (solid lines) and rCT (dashed lines).